# Light Higgs boson discovery in the Standard Model and beyond

J. A. Aguilar-Saavedra

Departamento de Física Teórica y del Cosmos and CAFPE, Universidad de Granada, E-18071 Granada, Spain

#### Abstract

We evaluate the LHC discovery potential for a light Higgs boson in  $t\bar{t}H$  ( $\rightarrow$  $\ell\nu bbbbjj$ ) production, within the Standard Model and if a new Q=2/3 quark singlet T with a moderate mass exists. In the latter case, T pair production with decays  $T\bar{T} \to W^+ b H \bar{t}$ ,  $H t W^- \bar{b} \to W^+ b W^- \bar{b} H$  provides an important additional source of Higgs bosons giving the same experimental signature. Both analyses are carried out with particle-level simulations of signals and backgrounds. Our estimate for SM Higgs discovery in  $t\bar{t}H$  production,  $2.25\sigma$  significance for  $M_H=115$ GeV and an integrated luminosity of  $30 \text{ fb}^{-1}$ , is more pessimistic than previous ones. We show that, if a quark singlet with a mass  $m_T = 500$  GeV exists, the luminosity required for Higgs discovery in this final state is reduced by a factor of 25, and  $5\sigma$  significance can be achieved already with 6 fb<sup>-1</sup>. This new Higgs signal will not be seen unless we look for it: with this aim, a new specific final state reconstruction method is presented. Finally, we consider the sensitivity of this decay mode of the  $T\bar{T}$  pair to search for Q=2/3 singlets. Combined with the  $T\bar{T} \to W^+bW^-\bar{b}$  mode, it allows to discover a 500 GeV quark with only 1.2  $fb^{-1}$  of luminosity.

## 1 Introduction

The discovery of the Higgs boson is one of the main goals of the Large Hadron Collider (LHC). Our present understanding of electroweak symmetry breaking in the Standard Model (SM) relies on the existence of at least one of such scalar particles [1], whose mass is however not predicted. Direct searches at LEP have placed the limit  $M_H > 114.4$  GeV on the mass of a SM-like Higgs, with a 95% confidence level (CL) [2]. Actually, data taken from the ALEPH collaboration showed an excess of events over the SM background consistent with a 115 GeV Higgs boson, but these results were not confirmed by the other LEP collaborations. There is some theoretical prejudice leading us to believe in the existence of a Higgs boson not much heavier than this direct bound. Precision electroweak data seem to indicate its existence, with a best-fit value of  $M_H = 91^{+45}_{-32}$  GeV for its mass [3] if the SM is assumed. On the other hand,

the Higgs boson must be lighter than around 1 TeV if the SM is required to remain perturbative up to the unification scale [4].

There is a vast Higgs search program at LHC, including various production processes and the decay channels relevant in each mass range [5,6]. Most analyses focus on the search of a SM-like Higgs boson. For masses  $M_H \lesssim 130$  GeV, the decay  $H \to b\bar{b}$  dominates, with a branching fraction around 0.9. However, the most important production process  $gg \to H$  is not visible in this channel due to the enormous QCD background. One has then to fall back either on rare decay modes, production processes in association with extra particles, or both. One example is the production together with a  $t\bar{t}$  pair, with  $H \to b\bar{b}$  and semileptonic decay of t,  $\bar{t}$ . Further examples are  $gg \to H$  followed by  $H \to \gamma\gamma$  (which has a branching ratio around 0.2%), or associate production  $t\bar{t}H$ , WH, ZH with  $H \to \gamma\gamma$ . It has been estimated that the first one allows to achieve  $5\sigma$  significance for a 120 GeV Higgs boson with an integrated luminosity of  $100~{\rm fb}^{-1}$  [5], while the combination of H,  $t\bar{t}H$ , WH and ZH production, with  $H \to \gamma\gamma$ , gives  $5\sigma$  already with 60 fb<sup>-1</sup>. Additionally, the latter decay channel provides a much more precise measurement of the Higgs mass.

For larger Higgs masses the prospects are better. For  $130 \lesssim M_H \lesssim 2M_W$ ,  $gg \to H$  production with decay  $H \to ZZ^* \to \ell^+\ell^-\ell'^+\ell'^-$  provides a very clean experimental signature of four charged leptons. A Higgs particle with  $M_H = 130$  GeV may be detected in this channel with 15 fb<sup>-1</sup>, and for  $M_H = 150$  GeV the luminosity required is reduced to 3 fb<sup>-1</sup>. For slightly larger masses,  $2M_W \lesssim M_H < 2M_Z$ , this mode gets very suppressed due to the appearance of the on-shell decay  $H \to W^+W^-$ . The latter, with  $W^+W^- \to \ell^+\nu\ell'^-\nu$ , gives  $5\sigma$  significance for a luminosity around 8 fb<sup>-1</sup> in this mass range. For masses larger than  $2M_Z$ , the mode  $H \to ZZ$  is possible with both Z bosons on their mass shell. This channel alone can signal the existence of a Higgs boson with a luminosity ranging from 1.8 fb<sup>-1</sup> for  $M_H = 200$  GeV to 12 fb<sup>-1</sup> for  $M_H = 600$  GeV. Larger masses up to approximately 1 TeV can be probed combining different channels.

In SM extensions these production mechanisms can be enhanced or suppressed, and new ones may appear. An interesting example takes place in Little Higgs models, where the  $gg \to H$  cross section may be suppressed but the branching ratio for  $H \to \gamma \gamma$  can increase, due to the extra contribution of the new fermions (including a Q = 2/3 quark singlet T) to the effective Hgg and  $H\gamma\gamma$  vertices [7]. Furthermore, a new production mechanism [8], very important for moderate masses of the new quark, is given by the decays  $T \to Ht$ . This possibility would be especially welcome, since it increases the observability of a Higgs boson in the mass region  $M_H \lesssim 130$  GeV where its detection is more difficult. In this work we focus on the latter, comparing the discovery potential

for a Higgs boson (for which we assume a mass of 115 GeV) within the SM and if a Q = 2/3 quark singlet exists. Our analysis applies to several SM extensions where such singlets appear, not only Little Higgs models [9] but also in extra-dimensions [10], and grand unified theories [11]. The process relevant for Higgs discovery is

$$gg, q\bar{q} \to T\bar{T} \to W^+bH\bar{t}, HtW^-\bar{b} \to W^+bW^-\bar{b}H,$$
 (1)

with semileptonic decay of the W pair and  $H \to b\bar{b}$ . It gives the same experimental signature  $\ell\nu b\bar{b}b\bar{b}jj$  as SM  $t\bar{t}H$  production but the kinematics is rather different. We compare the discovery potential in this final state within the SM (in which case the only signal is  $t\bar{t}H$ ) and with a new singlet T, assuming for its mass a reference value  $m_T = 500$  GeV. It has been shown that such a particle could be seen at LHC in a short time, through its decays  $T\bar{T} \to W^+bW^-\bar{b}$  [12]. Experimental search in the channel of Eq. (1) would improve the statistical significance of the T signal and, what is perhaps even more important, it would allow a prompt discovery of the Higgs boson.

# 2 Summary of the model

SM extensions with vector-like quarks under  $SU(2)_L$  have been introduced before, and their phenomenology has been extensively explored [13–16]. Here we will briefly recall the main features of a SM extension with a Q=2/3 quark singlet, summarising the most relevant points for this work. The addition of two  $SU(2)_L$  singlet fields  $T_{L,R}^0$  to the quark spectrum modifies the weak and scalar interactions involving Q=2/3 quarks. (We denote weak eigenstates with a zero superscript, to distinguish them from mass eigenstates which do not bear superscripts.) Using standard notation, these interactions read

$$\mathcal{L}_{W} = -\frac{g}{\sqrt{2}} \left[ \bar{u} \gamma^{\mu} V P_{L} d W_{\mu}^{+} + \bar{d} \gamma^{\mu} V^{\dagger} P_{L} u W_{\mu}^{-} \right] ,$$

$$\mathcal{L}_{Z} = -\frac{g}{2c_{W}} \bar{u} \gamma^{\mu} \left[ X P_{L} - \frac{4}{3} s_{W}^{2} \mathbb{1}_{4 \times 4} \right] u Z_{\mu} ,$$

$$\mathcal{L}_{H} = \frac{g}{2M_{W}} \bar{u} \left[ \mathcal{M}^{u} X P_{L} + X \mathcal{M}^{u} P_{R} \right] u H ,$$
(2)

where u = (u, c, t, T), d = (d, s, b) and  $P_{R,L} = (1 \pm \gamma_5)/2$ . The extended Cabibbo-Kobayashi-Maskawa (CKM) matrix V is of dimension  $4 \times 3$ ,  $X = VV^{\dagger}$  is a non-diagonal  $4 \times 4$  matrix and  $\mathcal{M}^u$  is the  $4 \times 4$  diagonal up-type quark mass matrix. The new mass eigenstate T is expected to couple mostly with third generation quarks t, b, because  $T_L^0$ ,  $T_R^0$  preferrably mix with  $t_L^0$ ,  $t_R^0$ , respectively, due to the large top quark mass.  $V_{Tb}$  is mainly constrained by the contribution of the new quark to the T parameter [16]. For  $m_T = 500$  GeV, the experimental measurement  $T = 0.12 \pm 0.10$  [17] implies  $|V_{Tb}| \leq 0.26$ 

with a 95% CL [12, 18]. Mixing of  $T_L^0$  with  $u_L^0$ ,  $c_L^0$ , especially with the latter, is very constrained by parity violation experiments and the measurement of  $R_c$  and  $A_{\rm FB}^{0,c}$  at LEP, respectively [14, 19], implying small  $X_{uT}$ ,  $X_{cT}$ . The charged current couplings with d, s must be small as well,  $|V_{Td}|, |V_{ts}| \sim 0.05$ , because otherwise the new quark would give large loop contributions to kaon and B physics observables [16]. Therefore,  $|V_{Td}|, |V_{Ts}| \ll |V_{Tb}|$  and  $|X_{uT}|, |X_{cT}| \ll |X_{tT}|$ , and the relevant decays of the new quark are  $T \to W^+b$ , Zt, Ht, with partial widths

$$\Gamma(T \to W^{+}b) = \frac{\alpha}{16 s_{W}^{2}} |V_{Tb}|^{2} \frac{m_{T}^{3}}{M_{W}^{2}} \left[ 1 - 3 \frac{M_{W}^{4}}{m_{T}^{4}} + 2 \frac{M_{W}^{6}}{m_{T}^{6}} \right] ,$$

$$\Gamma(T \to Zt) = \frac{\alpha}{16 s_{W}^{2} c_{W}^{2}} |X_{tT}|^{2} \frac{m_{T}^{2}}{M_{Z}^{2}} f(m_{T}, m_{t}, M_{Z})$$

$$\times \left[ 1 + \frac{M_{Z}^{2}}{m_{T}^{2}} - 2 \frac{m_{t}^{2}}{m_{T}^{2}} - 2 \frac{M_{Z}^{4}}{m_{T}^{4}} + \frac{m_{t}^{4}}{m_{T}^{4}} + \frac{M_{Z}^{2} m_{t}^{2}}{m_{T}^{4}} \right] ,$$

$$\Gamma(T \to Ht) = \frac{\alpha}{16 s_{W}^{2}} |X_{tT}|^{2} \frac{m_{T}^{2}}{M_{W}^{2}} f(m_{T}, m_{t}, M_{H})$$

$$\times \left[ 1 + 6 \frac{m_{t}^{2}}{m_{T}^{2}} - \frac{M_{H}^{2}}{m_{T}^{2}} + \frac{m_{t}^{4}}{m_{T}^{4}} - \frac{m_{t}^{2} M_{H}^{2}}{m_{T}^{4}} \right] ,$$
(3)

The kinematical function

$$f(m_T, m_t, M) \equiv \frac{1}{2m_T} (m_T^4 + m_t^4 + M^4 - 2m_T^2 m_t^2 - 2m_T^2 M^2 - 2m_t^2 M^2)^{1/2}$$
 (4)

approximately equals  $m_T/2$  for  $m_T\gg m_t, M$ . The two couplings  $V_{Tb}$ ,  $X_{tT}$  involved in the decays are related by  $|X_{tT}|^2\simeq |V_{Tb}|^2(1-|V_{Tb}|^2)$  and, for the values allowed by the T parameter, they are approximately equal. With the three partial widths proportional to  $|V_{Tb}|^2$ , the relative branching ratios only depend on  $m_T$  and  $M_H$ . For  $m_T=500$  GeV,  $M_H=115$  GeV we have  ${\rm Br}(T\to W^+b)=0.503$ ,  ${\rm Br}(T\to Zt)=0.166$ ,  ${\rm Br}(T\to Ht)=0.331$ . (We take  $V_{Tb}=0.2$ , for which the total T width is  $\Gamma_T=3.115$ .) The decays  $T\to Zt\to \ell^+\ell^-W^+b$ ,  $\ell=e,\mu$  give a cleaner final state than  $T\to W^+b$ , but with a branching ratio 10 times smaller. The channel  $T\to W^+b$  ( $\bar T\to W^-\bar b$ ) gives the best discovery potential for the new quark in single T [20] as well as in  $T\bar T$  production [12]. The remaining decay  $T\to Ht$  constitutes a copious source of Higgs bosons for moderate T masses, for which the  $T\bar T$  production cross section is large.

## 3 Signal and background simulation

Many SM and some new physics processes give or mimic the experimental signature studied of a charged lepton, four *b*-tagged jets, at least two additional jets and missing energy. The relevant processes are calculated with matrix-element-based Monte Carlo

generators and feeded into PYTHIA 6.228 [21] to include initial and final state radiation (ISR, FSR) and perform hadronisation. For the production of W and Z bosons plus six jets, or a  $b\bar{b}$  /  $c\bar{c}$  pair and four jets, we use ALPGEN [22]. For  $T\bar{T}$ ,  $t\bar{t}$ ,  $t\bar{t}H$ ,  $t\bar{t}b\bar{b}$  and  $t\bar{t}c\bar{c}$  (through QCD and electroweak (EW) interactions) and  $Wb\bar{b}b\bar{b}$  production, plus other processes obtained replacing the top quarks by heavy T quarks, we have developed Monte Carlo generators which use the full resonant tree-level matrix elements for the production and decay processes, namely

$$gg, q\bar{q} \to T\bar{T} \to W^{+}b H\bar{t}, Ht W^{-}\bar{b} \to W^{+}bW^{-}\bar{b}H \to f_{1}\bar{f}'_{1}b\bar{f}_{2}f'_{2}\bar{b} b\bar{b}/c\bar{c},$$

$$gg, q\bar{q} \to T\bar{T} \to W^{+}b Z\bar{t}, Zt W^{-}\bar{b} \to W^{+}bW^{-}\bar{b}Z \to f_{1}\bar{f}'_{1}b\bar{f}_{2}f'_{2}\bar{b} b\bar{b}/c\bar{c},$$

$$gg, q\bar{q} \to t\bar{t} \to W^{+}bW^{-}\bar{b} \to f_{1}\bar{f}'_{1}b\bar{f}_{2}f'_{2}\bar{b},$$

$$gg, q\bar{q} \to t\bar{t}H \to W^{+}bW^{-}\bar{b}H \to f_{1}\bar{f}'_{1}b\bar{f}_{2}f'_{2}\bar{b} b\bar{b}/c\bar{c},$$

$$gg, q\bar{q} \to t\bar{t}b\bar{b} \to W^{+}bW^{-}\bar{b}b\bar{b} \to f_{1}\bar{f}'_{1}b\bar{f}_{2}f'_{2}\bar{b} b\bar{b},$$

$$gg, q\bar{q} \to t\bar{t}c\bar{c} \to W^{+}bW^{-}\bar{b}c\bar{c} \to f_{1}\bar{f}'_{1}b\bar{f}_{2}f'_{2}\bar{b} c\bar{c},$$

$$q\bar{q}' \to W^{\pm}b\bar{b}b\bar{b} \to f_{1}\bar{f}'_{1}b\bar{b}b\bar{b}.$$

$$(5)$$

Matrix elements are calculated with HELAS [26], partly using MadGraph [27]. All finite width and spin effects are thus automatically taken into account. The colour flow information necessary for PYTHIA is obtained following the same method as in AcerMC [28]. i.e. we randomly select the colour flow among the possible ones on an event-by-event basis, computing the probabilities of a given configuration from the matrix element (taking into account the diagrams contributing to such configuration). Integration in phase space is done with VEGAS [29], modified following Ref. [28]. These generators (except  $Wb\bar{b}b\bar{b}$ ) have been cheched against ALPGEN using the same parameters, structure functions and factorisation scales, obtaining very good agreement. For our evaluations we take  $m_t = 175 \text{ GeV}$ ,  $m_b = 4.8 \text{ GeV}$ ,  $m_c = 1.5 \text{ GeV}$  ( $m_c$  is neglected in W decays)  $\alpha(M_Z) = 1/128.878$ ,  $s_W^2(M_Z) = 0.23113$ ,  $\alpha_s(M_Z) = 0.127$  and run the coupling constants up to the scale of the heavy (t or T) quark. Structure functions CTEQ5L [30] are used, with  $Q^2 = \hat{s}$  the square of the partonic centre of mass energy. (For ALPGEN processes we select  $Q^2 = M_{W,Z}^2 + p_{t_{W,Z}}^2$ .) Several representative total cross sections (without decay branching ratios nor phase space cuts) obtained can be found in Table 1, for comparison with other generators. The total cross sections for  $t\bar{t}c\bar{c}$  are numerically very unstable and not shown.

In our analysis we consider semileptonic decays of the  $W^+W^-$  pairs, and leptonic decays in the production of W/Z+ jets. The main contributions come from  $\ell=e,\mu$ , but decays to  $\tau$  leptons are included as well. Phase space cuts are applied at the generator level in some processes to reduce statistical fluctuations and improve the

Process	$\sigma_{ m tot}$	
$tar{t}$	$461~\mathrm{pb}$	
$Tar{T}$	2.14 pb	
$t ar{t} H$	508  fb	
$t ar{t} b ar{b}$	$8.65~\mathrm{pb}$	
$t\bar{t}b\bar{b}$ (EW)	$773~\mathrm{fb}$	
$Wbar{b}bar{b}$	303.4  fb	

Table 1: Total cross sections for several processes studied.

unweighting efficiency. The cuts applied are

$$\begin{split} t\bar{t}b\bar{b}, t\bar{t}c\bar{c}, Wb\bar{b}b\bar{b} & |\eta^{b,c}| \leq 2.5 \;,\; p_t^{b,c} \geq 15 \; \text{GeV} \\ Wb\bar{b}jjjj, Wc\bar{c}jjjj, Wjjjjjjj & |\eta^{\ell,b,j}| \leq 2.5 \;,\; p_t^{\ell} \geq 6 \; \text{GeV} \;,\; p_t^{b,j} \geq 15 \; \text{GeV} \;, \\ & \Delta R^{jj,bb} \geq 0.4 \;,\; \Delta R^{\ell j,\ell b} \geq 0.4 \\ Zb\bar{b}jjjj, Zc\bar{c}jjjj, Wjjjjjjj & |\eta^{b,j}| \leq 2.5 \;,\; p_t^{\ell,\max} \geq 6 \; \text{GeV} \;,\; p_t^{b,j} \geq 15 \; \text{GeV} \;, \\ & \Delta R^{jj,bb} \geq 0.4 \;, \end{split}$$

where  $\eta$  is the pseudorapidity,  $p_t$  the transverse momentum and  $\Delta R \equiv \sqrt{(\Delta \eta)^2 + (\Delta \phi)^2}$  the lego-plot distance. The cross sections after decay, including generator cuts, can be read in Table 2 for  $\ell = e, \mu$ . The  $T\bar{T}$  processes in Eqs. (5) with  $\bar{T}$  (or T) decaying to  $H\bar{t}, Z\bar{t}$  (Ht, Zt) will from now on be denoted as  $T\bar{t}H$ ,  $T\bar{t}Z$  for brevity.

The generated events are passed through PYTHIA as external processes to include ISR, FSR and perform hadronisation.<sup>1</sup> We use the standard PYTHIA settings except for b fragmentation, in which we use the Peterson parameterisation with  $\epsilon_b = -0.0035$  [31]. Tau leptons in the final state are decayed using TAUOLA [23] and PHOTOS [24]. A fast detector simulation ATLFAST 2.60 [25], with standard settings, is used for the modelling of the ATLAS detector. We reconstruct jets using a cone algorithm with  $\Delta R = 0.4$ . We do not apply trigger inefficiencies and assume a perfect charged lepton identification. The package ATLFASTB is used to recalibrate jet energies and perform b tagging, for which we select a 60% efficiency at the low luminosity run. The hadronised events are required to fulfill these two criteria: (a) the presence of one (and only one) isolated charged lepton, which must have transverse momentum  $p_t \geq 20$  GeV (for electrons),  $p_t \geq 6$  GeV (for muons) and  $|\eta| \leq 2.5$ ; (b) at least six jets with  $p_t \geq 15$  GeV,  $|\eta| \leq 2.5$ , with exactly four b tags. The signal and background efficiencies after these requirements are shown in Table 2.

In order to avoid double counting, in the PYTHIA simulation of the  $t\bar{t}$  and W/Z+6 jets processes we turn off  $b\bar{b}$  and  $c\bar{c}$  pair radiation, which are independently generated. Similarly, for  $t\bar{t}c\bar{c}$  and  $W/Z+b\bar{b}/c\bar{c}+4$  jets we turn off  $b\bar{b}$  pair radiation.

	-	
$T \bar{t} H$	$211.2~\mathrm{fb}$	5.8%
t ar t H	$144.4~{\rm fb}$	4.5%
$t ar{t}$	136.6 pb	0.047%
$t ar{t} b ar{b}$	$564.9~\mathrm{fb}$	4.6%
$t ar{t} c ar{c}$	$630.5~\mathrm{fb}$	0.64%
$t\bar{t}b\bar{b}~{ m EW}$	$60.31~\mathrm{fb}$	4.8%
$t\bar{t}c\bar{c}~{ m EW}$	$17.12~\mathrm{fb}$	0.75%
Wjjjjjj	$69.85~\mathrm{pb}$	$\sim 4.7 \times 10^{-6}$
$Wbar{b}jjjj$	$2.825~\mathrm{pb}$	0.11%
$Wcar{c}jjjj$	$3.279~\mathrm{pb}$	$\sim 0.011\%$
$W b ar{b} b ar{b}$	$2.587~\mathrm{fb}$	$\sim 1.1~\%$
Zjjjjjj	10.48 pb	$\sim 2.0\times 10^{-6}$
$Zbar{b}jjjj$	$722.5~\mathrm{fb}$	0.065%
$Zcar{c}jjjj$	$738.5~\mathrm{fb}$	$\sim 0.018\%$
$T \bar{t} Z$	29.03  fb	4.3%
$T \bar{T} b \bar{b}$	$1.054~\mathrm{fb}$	3.9%

eff

Process

Table 2: Cross section at the generator level and efficiency for signal and background processes in the decay channels with  $\ell=e,\mu$ . The corresponding cross sections for final states with tau leptons are approximately one half, with efficiencies 20-30 times smaller.

Finally, we must note that our calculation of the  $Wb\bar{b}b\bar{b}jj$  background, with  $Wb\bar{b}b\bar{b}$  production at the generator level and extra jet radiation performed by PYTHIA, must be regarded as an estimate. The reason is that in  $Wb\bar{b}b\bar{b}$  only  $q\bar{q}'$  scattering processes are involved, while gluon fusion contributes to  $Wb\bar{b}b\bar{b}jj$ . At any rate, this background turns out to be completely negligible.  $Zb\bar{b}b\bar{b}$  production has an even smaller cross section and we have not included it in our calculations. One may also think about  $T\bar{T}H$  production, with  $T\bar{T} \to W^+bW^-\bar{b}$ , also contributing to the final state studied. The Yukawa coupling of the T quark is very small,  $y_{HTT} = m_T/2M_W X_{TT}$ , with  $X_{TT} = |V_{Tb}|^2 = 0.04$ , and this process is irrelevant.

# 4 Higgs boson discovery

We simulate events for an integrated luminosity of 30 fb<sup>-1</sup>, which can be collected in three years at the low luminosity phase. For each process, the number of events simulated corresponds to the cross section obtained from the generator scaled by a K factor, defined as in Ref. [12]. These K factors approximately take into account

higher order processes with extra jets from FSR. With this prescription, our "rescaled"  $t\bar{t}X \to \ell^{\pm}\nu b\bar{b}jjX$  cross section, for instance, is of 172 pb, close to the PYTHIA value of 189 pb [32]. The number of events generated for each process can be read in Table 3. In the sums, the first term corresponds to final states with  $\ell = e, \mu$  and the second one to  $\ell = \tau$ . A subtlety in the analysis is that when the singlet T is introduced the Htt, Wtb and Ztt couplings of the top quark are modified. This affects electroweak  $t\bar{t}b\bar{b}$  and  $t\bar{t}c\bar{c}$  production in a non-trivial way, and different samples (taking into account the corrections to the couplings) must be generated and simulated.  $t\bar{t}H$  production is modified as well, with the Yukawa coupling of the top quark reduced by a factor  $X_{tt} < 1$ . In our case, we have assumed a large mixing  $V_{Tb} = 0.2$ , for which  $|V_{tb}| = 0.98$  and  $X_{tt} = 0.96$ . These processes are indicated with a "(T)" in Table 3, where we can observe that the effect of mixing is negligible for  $t\bar{t}b\bar{b}$  and  $t\bar{t}c\bar{c}$ . A second issue to keep in mind is that when studying the new physics signals associated to the T quark we must distinguish the cases where the Higgs boson is present or not (if not, the branching ratios for  $T \to W^+b$  and  $T \to Zt$  are larger). The latter are denoted with a "(H)".

We perform two different analyses of signals and backgrounds. The first one is a "standard" analysis aiming to discover the Higgs boson in  $t\bar{t}H$  production, in which we reconstruct the final state to distinguish this signal from the SM background. In case that a new quark T exists, there will be additional signal events improving the Higgs discovery potential. The second analysis specifically looks for a Higgs boson produced in heavy quark decays, optimising the reconstruction for this signal.

#### 4.1 Analysis I: $t\bar{t}H$ reconstruction

Before analysing the Higgs discovery potential in this channel, we must comment a few aspects about the observability of  $t\bar{t}H$  production. The uncertainty in the background normalisation makes it difficult to detect the presence of a Higgs boson with a measurement of the total  $\ell\nu bbbbjj$  cross section. Naively, from the data in Table 3 one could conclude that the statistical significance of the  $t\bar{t}H$  signal, before applying any kinematical cut, is  $S/\sqrt{B}=254.1/\sqrt{4300.7}=3.87$ . However, this estimate does not include the systematic uncertainty in the SM background total cross section (i.e. the background normalisation). Assuming a 5% uncertainty (which seems rather optimistic in the case of total cross sections) and adding statistical and systematic uncertainties in quadrature, we obtain a much smaller significance of 1.13. The discovery of the  $t\bar{t}H$  signal may be done with the identification of a "Higgs" peak in a  $b\bar{b}$  invariant mass distribution: the SM background normalisation (for which we will assume in the following a 5% uncertainty) can be achieved with actual measurements of real data away from the peak, and the Higgs signal is seen as a peak over the expected background. In this

	$N_0$	N
$Tar{t}H$	$8360^* + 4180^*$	482.9 + 18.1
$t ar{t} H$	$5460^* + 2720^*$	244.3 + 8.1
$t \bar{t} H$ $(T)$	$5030^* + 2510^*$	227.8 + 7.3
$t \overline{t}$	5160000 + 2580000	2445 + 70
$t ar{t} b ar{b}$	24900 + 12500	1145 + 35
$t \bar{t} b \bar{b}  { m EW}$	$2660^* + 1330^*$	127.8 + 4.2
$t\bar{t}b\bar{b} \ {\rm EW} \ (T)$	$2460^* + 1230^*$	126.8 + 3.6
$tar{t}car{c}$	27800 + 13900	177 + 7
$t\bar{t}c\bar{c}$ EW	$755^* + 378^*$	5.3 + 0.1
$t\bar{t}c\bar{c} \ \mathrm{EW} \ (T)$	$702^* + 351^*$	4.2 + 0.0
$Wbar{b}jjjj$	168000 + 83900	181 + 7
$Wcar{c}jjjj$	195000 + 97400	21 + 0
Wjjjjjj	5270000 + 2640000	25 + 1
$W b ar{b} b ar{b}$	$118^* + 58.4^*$	1.3 + 0.0
$Zbar{b}jjjj$	53600 + 26800	35 + 1
$Zcar{c}jjjj$	54800 + 27400	10 + 0
Zjjjjjjj	1020000 + 510000	2 + 0
$Tar{t}Z$	$1150^* + 575^*$	50.0 + 2.1
$Tar{t}Z$ ( $ ot\!\!H$ )	$2570^* + 1280^*$	108.3 + 4.0
$T \bar{T} b \bar{b}$	$48.7^* + 23.8^*$	1.9 + 0.1
$Tar{T}bar{b}$ ( $ ot\!\!/I$ )	$109^* + 53.3^*$	5.0 + 0.3

Table 3: For each process: number of events simulated  $N_0$  and number of events passing the pre-selection criteria N. The first terms in the sums correspond to  $\ell = e, \mu$ , and the second ones to  $\ell = \tau$ . For some contributions (marked with an asterisk) we have simulated  $10N_0$  events and divided the result by 10, so as to reduce statistical fluctuations.

work we will use both estimators,

$$S_0 \equiv S/\sqrt{B} , \quad S_5 \equiv S/\sqrt{B + (0.05B)^2}, \qquad (7)$$

to calculate the statistical significance of the signals.

In order to reconstruct the Higgs mass we follow the procedure in Ref. [5], with minor changes. The W decaying hadronically is reconstructed from two non-b jets  $j_1$ ,  $j_2$ , which we select as:  $j_1$  is the one with highest  $p_t$ ;  $j_2$  is the one having with  $j_1$  an invariant mass  $M_W^{\text{had}}$  closest to  $M_W$ . We require  $M_W^{\text{had}}$  to be within an interval

$$M_W - 30 \text{ GeV} \le M_W^{\text{had}} \le M_W + 30 \text{ GeV},$$
 (8)

rejecting events with  $M_W^{\rm had}$  mass outside this interval, and then correct it to  $M_W$  by

an appropriate scaling of the two jet momenta. For the W decaying leptonically, the missing transverse momentum is assigned to the neutrino, and its longitudinal momentum and energy are found requiring that the invariant mass of the charged lepton and neutrino is the W mass,  $(p_{\ell} + p_{\nu})^2 = M_W^2$  (this equation gives two possible solutions). Among the four b jets, two originate from the t,  $\bar{t}$  decays and the other two correspond to the Higgs boson. We first identify the two b jets from t,  $\bar{t}$  as the ones yielding invariant masses  $m_t^{\text{had}}$ ,  $m_t^{\text{lep}}$  (of the top quark decaying hadronically and semileptonically, respectively) closest to the top mass, choosing among the 24 possible combinations the two b jets  $b_1$ ,  $b_2$  and neutrino momentum solution which minimise the quantity  $(m_{j_1j_2b_1} - m_t)^2 + (m_{\ell\nu b_2} - m_t)^2$ . The two remaining jets are then assigned to the Higgs boson. The kinematical distribution of these variables is shown in Fig. 1.

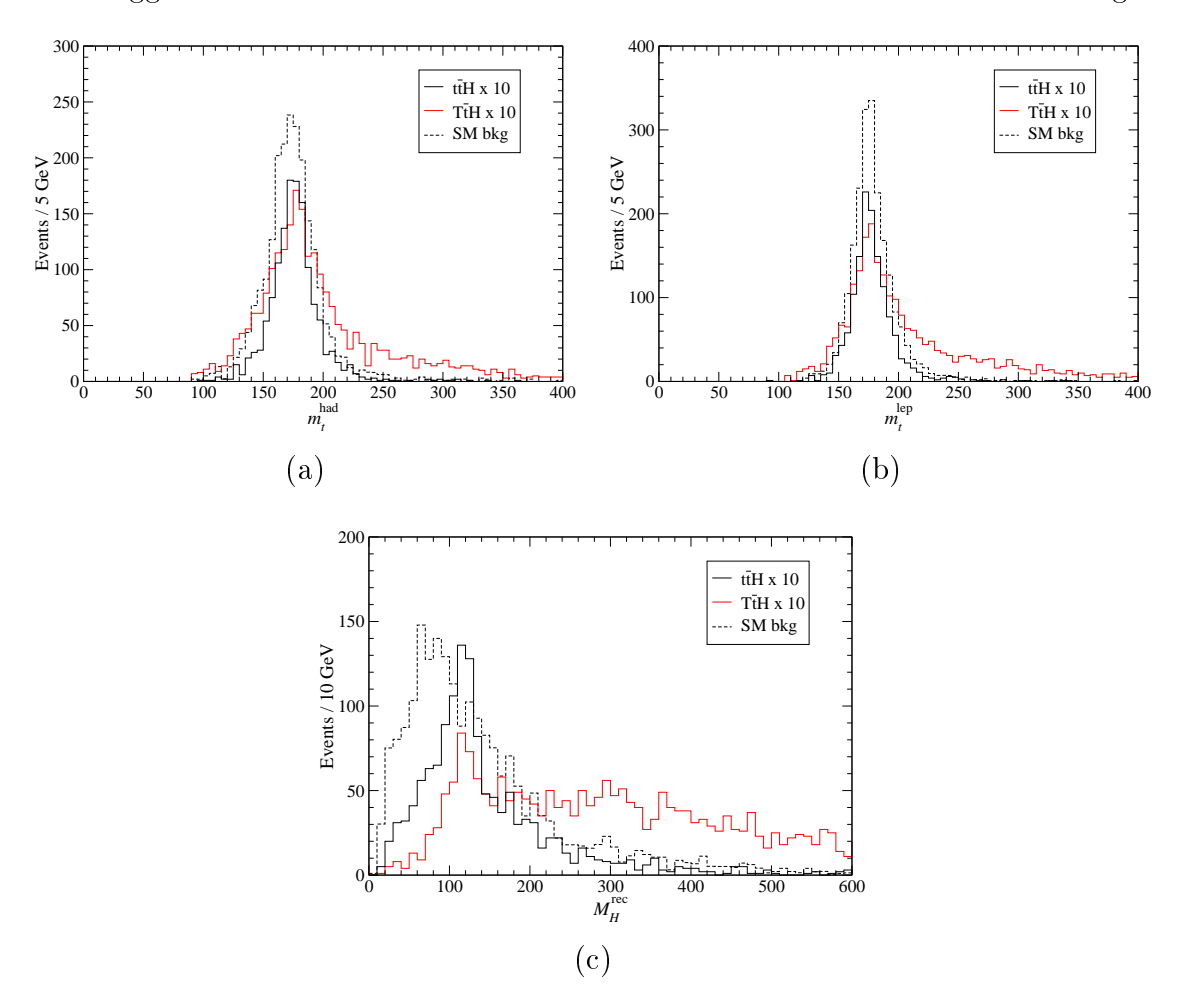


Figure 1: Analysis I: Reconstructed masses of the top quarks decaying (a) hadronically, and (b) semileptonically. Reconstructed Higgs mass (c). The plots include the kinematical cut in Eq. (8).

In addition to the cut on  $M_W^{\text{had}}$  mentioned before, we require  $m_t^{\text{had}}$  and  $m_t^{\text{lep}}$  within

intervals

$$m_t - 30 \text{ GeV} \le m_t^{\text{had}}, m_t^{\text{lep}} \le m_t + 30 \text{ GeV}.$$
 (9)

The kinematical distribution of the Higgs reconstructed mass after these selection criteria is shown in Fig. 2, for the SM background alone and the SM background plus  $t\bar{t}H$  production. The number of events corresponding to each process can be read in the first column of Table 4. The  $t\bar{t}H$  signal is barely observable as an excess of events around  $M_H^{\rm rec} = 115$  GeV. In the invariant mass window  $M_H^{\rm rec} = 115 \pm 20$  GeV, the excess of events has  $S_0 = 2.25$ ,  $S_5 = 1.69$ . The number of events in the peak region corresponding to each process can be found in the second column of Table 4. We also plot the distribution obtained in case that a 500 GeV quark singlet T exists, in which case  $t\bar{t}H$  production decreases, the SM background is slightly modified, and the  $T\bar{t}H$  signal and small additional backgrounds  $(T\bar{t}Z$  and  $T\bar{T}b\bar{b}$ ) are added.

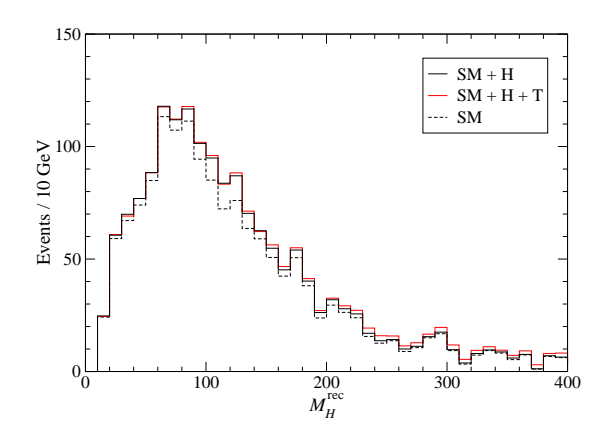


Figure 2: Analysis I: Reconstructed Higgs mass after the selection cuts in Eqs. (8,9). The dashed line represents the SM background, while the continuous lines also include: (i) the  $t\bar{t}H$  signal; (ii) the (modified)  $t\bar{t}H$  and  $T\bar{t}H$  signals and new backgrounds associated to the quark singlet.

It is worth comparing our results with the previous ones in Ref. [5]. In that study different invariant mass intervals are chosen, 25 GeV for the  $M_W^{\text{had}}$  cut, 20 GeV for  $m_t^{\text{had}}$ ,  $m_t^{\text{lep}}$  and 30 GeV for  $M_H^{\text{rec}}$ . (With these values we obtain  $\mathcal{S}_0 = 2.00$ ,  $\mathcal{S}_5 = 1.52$ .) In our analysis we find a smaller  $S/\sqrt{B}$  mainly because our background estimation is more than two times larger. The results obtained with a quark singlet also deserve further explanation. The Higgs signal from T decays is a factor of two larger than  $t\bar{t}H$  production, but it is strongly suppressed by the reconstruction procedure due to its very different kinematics (see Fig. 1). After selection cuts the remaining  $T\bar{t}H$  signal is very small, only 7.5 events, giving (after the decrease in  $t\bar{t}H$ ) a moderate improvement in the significance,  $\mathcal{S}_0 = 2.56$ ,  $\mathcal{S}_5 = 1.92$ . Clearly, a different analysis is needed to take advantage of the large number of Higgs bosons produced in T decays.

	$N_{ m cut}$	$N_{ m peak}$	
$Tar{t}H$	71.3 + 2.2	7.3 + 0.2	
$t ar{t} H$	103.7 + 4.3	38.2 + 1.5	
$t \bar{t} H \ (T)$	96.6 + 4.1	35.9 + 1.4	
$t ar{t}$	913 + 31	188 + 6	
$t ar{t} b ar{b}$	449 + 11	77 + 0	
$t \bar{t} b \bar{b}  { m EW}$	56.2 + 1.5	13.1 + 0.2	
$t\bar{t}b\bar{b} \text{ EW }(T)$	50.2 + 1.7	11.8 + 0.2	
$t ar{t} c ar{c}$	68 + 4	14 + 0	
$t\bar{t}c\bar{c}$ EW	2.2 + 0.1	0.4 + 0.0	
$t\bar{t}c\bar{c} \ \mathrm{EW} \ (T)$	1.3 + 0.0	0.2 + 0.0	
$Wbar{b}jjjj$	42 + 2	7 + 0	
W c ar c j j j j	5 + 0	1 + 0	
Wjjjjjj	8 + 0	1 + 0	
$Wbar{b}bar{b}$	0.3 + 0.0	0.2 + 0.0	
$Zbar{b}jjjj$	7 + 0	3 + 0	
$Zcar{c}jjjj$	4 + 0	0 + 0	
Zjjjjjj	1 + 0	1 + 0	
$Tar{t}Z$	6.9 + 0.2	0.4 + 0.0	
$T ar{T} b ar{b}$	0.2 + 0.0	0.0 + 0.0	

Table 4: Analysis I: number of events  $N_{\text{cut}}$  passing the selection cuts in Eqs. (8),(9); number of events  $N_{\text{peak}}$  passing the selection cuts which are in the Higgs peak region.

#### 4.2 Analysis II: $T\bar{t}H$ reconstruction

The reconstruction of  $T\bar{T} \to W^+b\,H\bar{t}$ ,  $Ht\,W^-\bar{b} \to W^+bW^-\bar{b}H$  decays is more involved than for  $t\bar{t}H$ . Nevertheless, there is one crucial aspect from the experimental point of view: the heavy quark mass does not need to be known, and only the fact that two particles T,  $\bar{T}$  with equal mass are produced is used for the reconstruction. We first identify the W boson decaying hadronically from two untagged jets, taken as before:  $j_1$  is the one with highest  $p_t$  and  $j_2$  the one having with  $j_1$  an invariant mass closest to  $M_W$ . In contrast with the analysis I, we do not apply any kinematical cut on  $M_W^{\rm had}$ , nor rescale it to  $M_W$ . The momentum of the W boson decaying leptonically is also determined as in the previous analysis, giving two possible solutions.

With the W momenta determined up to a twofold ambiguity, we identify the two heavy quarks. There are eight possibilities for the pairing, because: (i) the heavy quark decaying to Wb (irrespectively of whether it is T or  $\bar{T}$ ) may have the W boson decaying hadronically or leptonically; (ii) the b quark resulting from this decay may

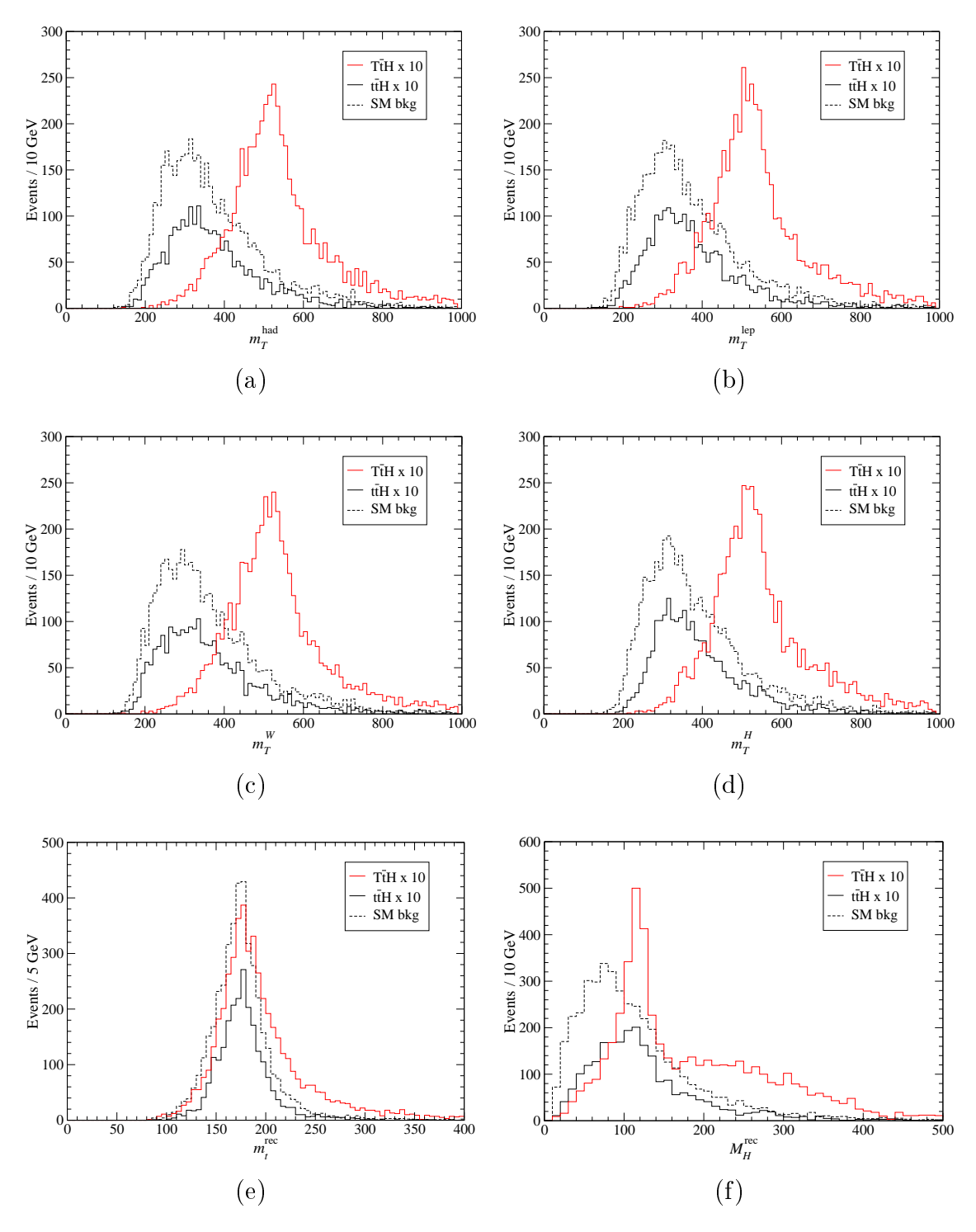


Figure 3: Analysis II: Reconstructed masses after pre-selection cuts of the heavy quarks T decaying hadronically (a), semileptonically (b), to  $W^+b/W^-\bar{b}$  (c), and to  $Ht/H\bar{t}$  (d). Reconstructed top (e) and Higgs mass (f).

correspond to each one of the four b-tagged jets in the final state. Among the 16 resulting possibilities, we select the one giving closest invariant masses for the two heavy quarks. The resulting distributions for the heavy quarks with hadronic and semileptonic decays are plotted in Fig. 3 (a) and (b). Both mass distributions include decays  $T \to W^+b$ ,  $T \to Ht$  as well as their charge conjugate. One can also consider the opposite: the invariant mass distributions  $m_T^W$ ,  $m_T^H$  of the heavy quarks decaying to Wb and to Ht, summing the charge conjugate channels and W hadronic and leptonic decays. These are plotted in Fig. 3 (c) and (d).

Once the  $T(\bar{T})$  quark decaying to  $Ht(H\bar{t})$  is identified (consisting of three b-tagged jets and a W boson), it only remains to find the b jet corresponding to the top quark. This jet is chosen as the one having with the W boson an invariant mass closest to  $m_t$ . The two remaining b jets are then assigned to the Higgs. The distributions of the top quark and Higgs boson reconstructed masses are presented in Fig. 3 (e) and (f). We can observe that the reconstruction procedure works quite well, especially if we bear in mind that we have to select between 48 possible combinations.

In this analysis we do not set "quality" cuts on the reconstructed heavy quark and top masses to enhance the signal. It would be very easy to do so from the experimental point of view, since the reconstructed masses peak at  $m_T$ , making the production of the  $T\bar{T}$  pair apparent (see next section). Instead, for simplicity we only exploit the fact that  $T\bar{T}$  events generically have very large transverse momenta. The total transverse energy  $H_t$  is an excellent choice, as can be noticed examining its distribution in Fig. 4 (a). We find useful to consider three more variables: the transverse momenta of the fastest jet and b jet,  $p_t^{j,\max}$  and  $p_t^{b,\max}$  respectively, and the transverse momentum of the b jet corresponding to the decay  $T \to W^+b$  ( $\bar{T} \to W^-\bar{b}$ ), denoted as  $p_t^{b,T}$ . The three variables are shown in Fig. 4 (b)–(d). The selection cuts applied to reduce the background are

$$H_t \ge 1000 \text{ GeV},$$
 $p_t^{j,\text{max}} \ge 200 \text{ GeV},$ 
 $p_t^{b,\text{max}} \ge 150 \text{ GeV},$ 
 $p_t^{b,T} \ge 50 \text{ GeV}.$  (10)

At this point it is important to draw attention to the fact that, since neither the T quark nor the Higgs boson have been discovered at present, there are two possible definitions for what we consider as signal and background. The first one would be to take as background just the SM processes in Table 3 (excluding  $t\bar{t}H$ ), and for the signal  $t\bar{t}H$ ,  $T\bar{t}H$ ,  $T\bar{t}Z$  and  $T\bar{T}b\bar{b}$ . The second possibility is to take as background the SM processes (slightly modified by the presence of the heavy quark) plus  $T\bar{t}Z$  and

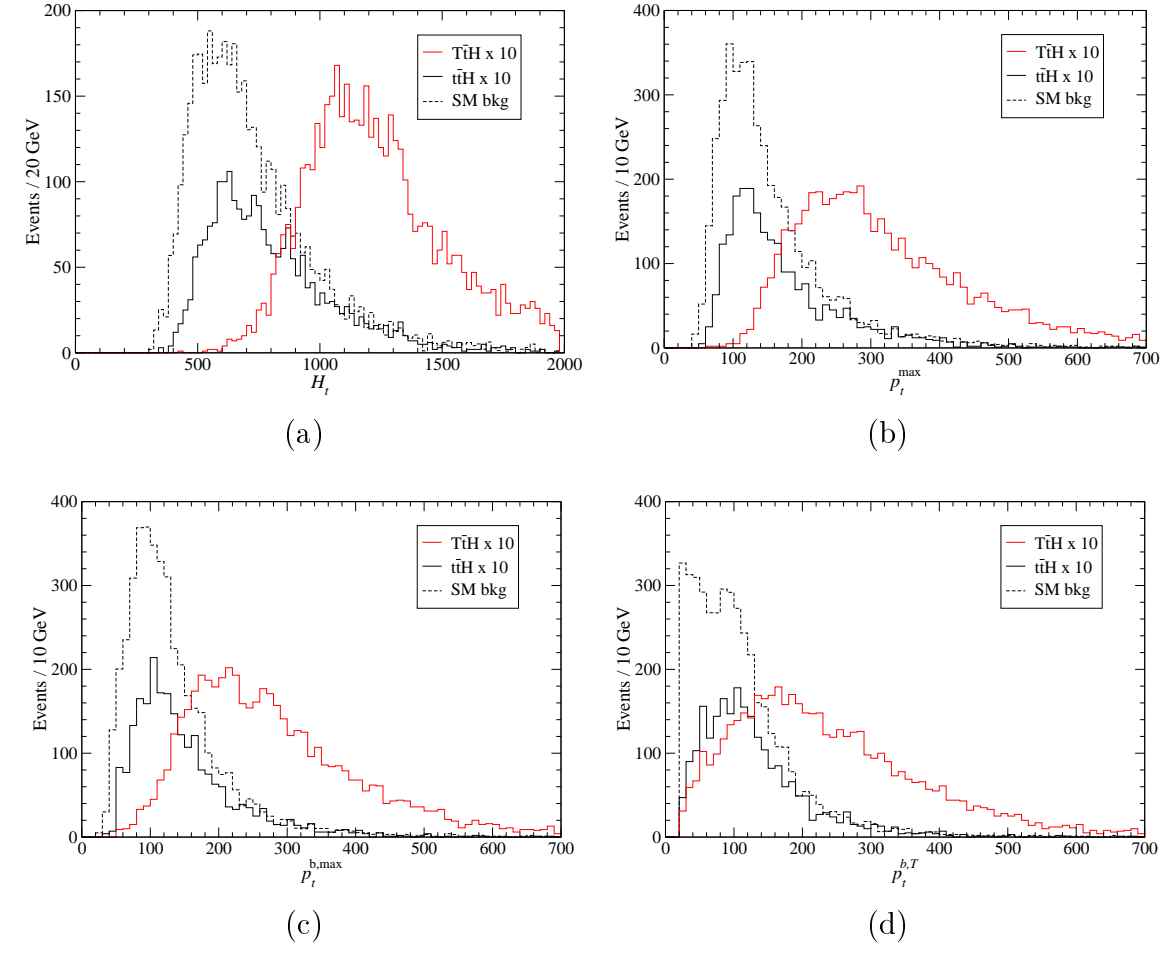


Figure 4: Analysis II: Total transverse energy (a), and transverse momentum of: the fastest jet (b); the fastest b-tagged jet (c); the b jet assigned to the  $T \to W^+b$  ( $\bar{T} \to W^-\bar{b}$ ) decay (d).

 $T\bar{T}b\bar{b}$  in the absence of a Higgs boson (see Table 3). Signal plus background is then constituted by the SM processes, plus  $T\bar{t}Z$  and  $T\bar{T}b\bar{b}$  with a Higgs boson,  $t\bar{t}H$  and  $T\bar{t}H$ . The "signal", that is, the excess of events over the background, is then  $t\bar{t}H$  plus  $T\bar{t}H$  minus the difference between  $T\bar{t}Z$  and  $T\bar{T}b\bar{b}$  without and with a Higgs boson. Both conventions lead to appreciably different results, and we adopt the latter, more conservative.<sup>2</sup> With this definition, we show in Fig. 5 the kinematical distribution of the reconstructed Higgs mass after the selection cuts in Eqs. (10), for the background alone and the background plus signal. The number of events corresponding to each process are collected in the first column of Table 5, and the numbers of events within

<sup>&</sup>lt;sup>2</sup>This amounts to considering that the T quark will have been discovered before the Higgs boson, what would indeed be the case for  $m_T = 500$  GeV, either in this final state or in the mode  $T\bar{T} \to W^+bW^-\bar{b}$ .

the window

$$80 \text{ GeV} \le M_H^{\text{rec}} \le 140 \text{ GeV} \tag{11}$$

are presented in the second column. (The numbers of events  $N'_{\text{peak}}$  in the heavy quark peak regions, without any cut on  $M_H^{\text{rec}}$ , are shown in the third column for later use.) They yield a statistical significance  $S_0 = 11.48$ ,  $S_5 = 10.16$  for the Higgs.<sup>3</sup> A  $5\sigma$  significance could be achieved with a luminosity of 6 fb<sup>-1</sup>, even allowing for a 5% uncertainty in the background normalisation. Comparing with the results for  $t\bar{t}H$  production alone in the previous subsection, the reduction in the luminosity required for discovery is a factor of 25.

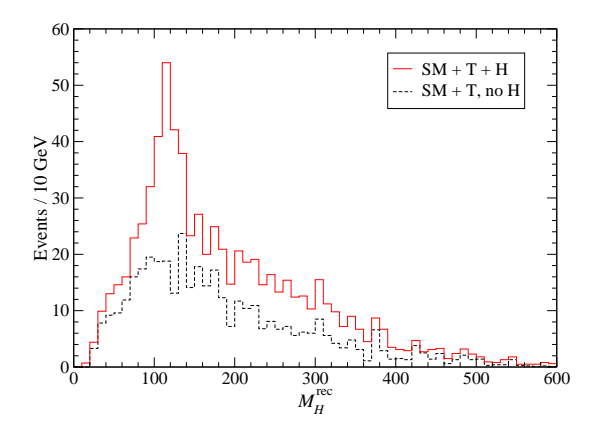


Figure 5: Analysis II: Reconstructed Higgs mass after the selection cuts in Eqs. (10). The dashed line represents the SM plus T background contributions in the absence of Higgs boson. The continuous line corresponds to SM background, T background contributions in the presence of a Higgs boson and Higgs signals.

#### 4.3 Other results

We conclude this section examining the dependence of our results on some of our assumptions. We estimate how our results change if: (i) we do not include the K factors mentioned at the beginning of this section; (ii) we use MRST structure functions [33]; (iii) we include the charged lepton identification efficiency; (iv) we select b tagging efficiencies of 50% or 70%. In the first and second cases, we compute the significances rescaling the numbers of events in Tables 4 and 5 by factors reflecting the change in the cross sections. In the third case we naively use an average charged lepton identification efficiency of 90%. For the latter two, we estimate the different acceptances from the

 $<sup>^{3}</sup>$ A higher significance is achieved without the cut in Eq. (11),  $\mathcal{S}_{0} = 16.22$ ,  $\mathcal{S}_{5} = 11.41$ , but the need of background normalisation suggests that it is more realistic to consider an adequate invariant mass window, which we take as in Eq. (11).

	$N_{ m cut}$	$N_{ m peak}$	$N_{ m peak}'$
$Tar{t}H$	326.1 + 12.1	119.4 + 3.7	221.1 + 7.3
$t ar{t} H$	33.4 + 1.2	10.2 + 0.2	18.3 + 0.8
$t\bar{t}H$ $(T)$	31.2 + 1.1	9.8 + 0.2	17.4 + 0.8
$t \overline{t}$	95 + 0	28 + 0	44 + 0
$t ar{t} b ar{b}$	142 + 5	37 + 1	74 + 4
$t \bar{t} b \bar{b}  \mathrm{EW}$	12.9 + 0.3	3.0 + 0.1	6.1 + 0.2
$t\bar{t}b\bar{b} \ \mathrm{EW} \ (T)$	15.4 + 0.5	3.6 + 0.1	8.6 + 0.3
$tar{t}car{c}$	22 + 1	7 + 1	8 + 1
$t\bar{t}c\bar{c}$ EW	0.8 + 0.0	0.0 + 0.0	0.6 + 0.0
$t\bar{t}c\bar{c} \ \mathrm{EW} \ (T)$	0.8 + 0.0	0.4 + 0.0	0.3 + 0.0
$Wbar{b}jjjj$	31 + 0	7 + 0	14 + 0
$Wcar{c}jjjj$	3 + 0	0 + 0	1 + 0
Wjjjjjj	4 + 0	1 + 0	1 + 0
$Wbar{b}bar{b}$	0.1 + 0.0	0.0 + 0.0	0.0 + 0.0
$Zbar{b}jjjj$	5 + 0	1 + 0	3 + 0
$Zcar{c}jjjj$	2 + 0	2 + 0	2 + 0
Zjjjjjj	0 + 0	0 + 0	0 + 0
$Tar{t}Z$	33.8 + 1.6	9.7 + 0.3	22.4 + 0.9
$Tar{t}Z$ $( ot\!\!H)$	72.7 + 3.1	20.7 + 0.8	47.6 + 1.8
$T ar{T} b ar{b}$	1.8 + 0.1	0.1 + 0.0	0.7 + 0.0
$Tar{T}bar{b}\;( ot\!\!/\!\!\!I)$	4.4 + 0.3	0.5 + 0.1	2.0 + 0.0

Table 5: Analysis II: number of events  $N_{\text{cut}}$  passing the selection cuts in Eqs. (10); number of events  $N_{\text{peak}}$  passing the selection cuts which are in the Higgs peak region; number of events  $N'_{\text{peak}}$  passing the selection cuts which are in the heavy quark peak regions.

nominal b tagging efficiencies and rejection factors. The resulting significances for the Higgs signals (only  $t\bar{t}H$  for the analysis I; the two signals for the analysis II) are collected in Table 6.

# 5 Heavy quark discovery

In this section we examine the discovery potential for Q=2/3 singlets in the  $\ell\nu bbbbjj$  decay mode, for a mass  $m_T=500$  GeV. The analysis is the same as in section 4.2, with the difference that here  $T\bar{t}Z$  (as well as  $T\bar{T}b\bar{b}$ ) production is a signal, while  $t\bar{t}H$  production (as predicted in the SM) constitutes a background. We also have to replace the electroweak  $t\bar{t}b\bar{b}$  and  $t\bar{t}c\bar{c}$  backgrounds by the SM predictions without the T quark

	Analysis I		Analysis I	
	$\mathcal{S}_0$	$\mathcal{S}_5$	$\mathcal{S}_0$	$\mathcal{S}_5$
Standard	2.25	1.69	11.48	10.16
K = 1	2.07	1.65	10.43	9.54
MRST	2.20	1.64	13.00	11.42
$\ell$ eff. $90\%$	2.13	1.63	10.89	9.74
b eff. $50%$	2.33	2.15	9.80	9.40
b eff. $70%$	1.43	0.52	8.33	4.96

Table 6: Estimates of the signal significances under different assumptions, explained in the text.

(the differences are negligible however, and seem a statistical effect). After the selection cuts in Eqs. (10), the mass distributions of the T quarks decaying hadronically and semileptonically are as shown in Fig. 6. Within a mass window

$$350 \text{ GeV} \le m_T^{\text{had}}, m_T^{\text{lep}} \le 650 \text{ GeV}$$
 (12)

the significance of the signal is  $S_0 = 18.81$ ,  $S_5 = 15.65$ . (The number of events corresponding to each process can be found in the first and third columns of Table 5.) It has been previously shown that the decay mode  $T\bar{T} \to W^+bW^-\bar{b}$  gives  $S_0 = 10.94$ ,  $S_5 = 7.69$  for 10 fb<sup>-1</sup> of integrated luminosity [12]. For the processes under study and the latter luminosity we have  $S_0 = 10.86$ ,  $S_5 = 10.13$ . Hence, for a heavy quark with  $m_T = 500$  GeV the two final states give practically the same significance, with a small advantage for  $\ell\nu bbjj$  final states. This will change of course if b tagging performance is better or worse than expected. Combining both channels, we obtain that a 500 GeV quark T can be discovered with 1.2 fb<sup>-1</sup> of luminosity.

# 6 Summary

Heavy singlet decays were early recognised as an important source of Higgs bosons [8], with a branching ratio close to 25%. In this work we have addressed the experimental observation at LHC, assuming a Higgs mass of 115 GeV and the possible existence of a 500 GeV heavy quark T. We have performed a detailed signal and background study, with matrix-element-based generators for the hard processes, subsequent parton showering and hadronisation by PYTHIA and a fast simulation of the ATLAS detector. As a by-product, new leading-order event generators for  $t\bar{t}$ ,  $t\bar{t}b\bar{b}$ ,  $t\bar{t}c\bar{c}$ ,  $t\bar{t}H$ ,  $Wb\bar{b}b\bar{b}$  and other processes have been developed. These generators include top quark, W and Higgs

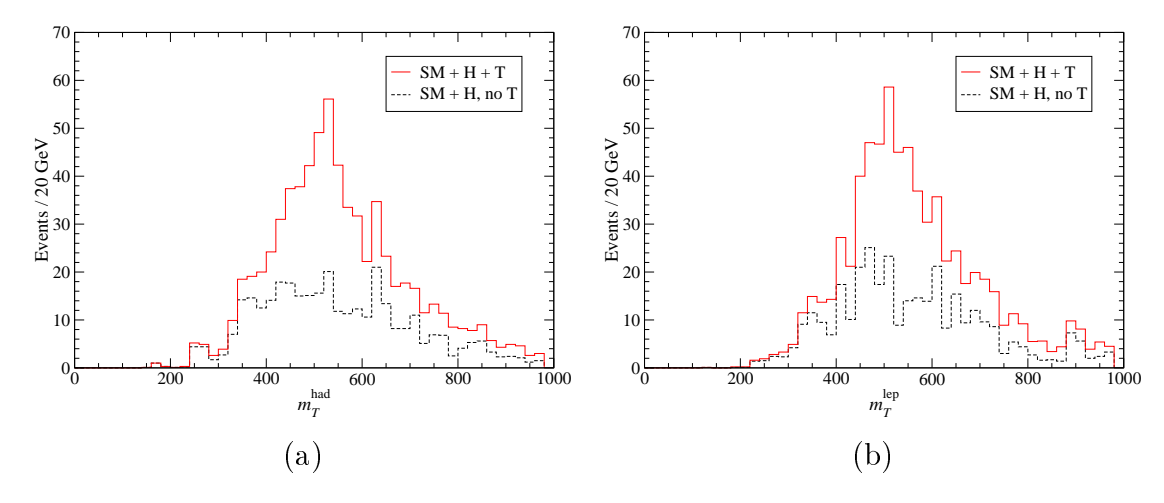


Figure 6: Reconstructed masses of the heavy quarks decaying hadronically (a) and semileptonically (b), after the selection cuts in Eqs. (10). The dashed line represents the SM background, and the continuous line corresponds to SM background plus T contributions.

boson decays and take finite width and spin effects into account. Their output provides the colour information necessary for hadronisation.

In our analysis we have first reevaluated the discovery potential of  $t\bar{t}H$  producion, with  $H\to b\bar{b}$  and semileptonic decay of the  $t\bar{t}$  pair, in the SM. Our result,  $S/\sqrt{B}=2.25$  for 30 fb<sup>-1</sup> at the low luminosity run, is more pessimistic than previous ones. The main reason is that in our simulations the SM background  $(t\bar{t}jj, t\bar{t}b\bar{b}, t\bar{t}c\bar{c}, Wb\bar{b}jjjj)$  and others) turns out to be a factor of two larger. The b tagging performance has a large impact on the final result, especially regarding the dominant  $t\bar{t}jj$  background. We have used the efficiencies implemented in ATLFASTB for the low luminosity run: 60% b tagging rate and nominal rejection factors of 6.7 for charm and 93 for light jets (with  $p_t$ -dependent corrections). If the latter are better than expected, the observability of  $t\bar{t}H$  production will improve. In this respect, full simulations of matrix-element-generated signals and backgrounds would be welcome.

The observability of the  $T\bar{T} \to W^+ b \, H\bar{t}, Ht\, W^- \bar{b} \to W^+ b W^- \bar{b} H$  signal has been then examined. We have demonstrated that, in a standard search for  $t\bar{t}H$  production, a possible contribution of this process can easily be overlooked, and improves very little the Higgs signal. We have presented a novel reconstruction technique specific for the search of this  $T\bar{t}H$  signal, which does not require the knowledge of the heavy quark mass. With this procedure, the  $T\bar{t}H$  process is cleanly separated from the SM background, giving a high statistical significance for the Higgs,  $S/\sqrt{B}=11.48$  for 30 fb<sup>-1</sup>. In case that a 500 GeV quark T exists, 6 fb<sup>-1</sup> of luminosity will suffice to discover the Higgs boson, assuming a 5% uncertainty in the background normalisation.

We have finally addressed the observability of the new quark, which is not equivalent to the discovery of the Higgs boson because the classification of processes as signals and background varies. We have shown that a significance  $S/\sqrt{B}=18.86$  is reached for 30 fb<sup>-1</sup>, practically the same as in the  $T\bar{T}\to W^+bW^-\bar{b}$  channel. Combining both, we find that  $5\sigma$  significance can be achieved with a luminosity of 1.2 fb<sup>-1</sup>, even allowing for a 5% systematic uncertainty in the background normalisation. For higher T masses,  $T\bar{T}W^+bW^-\bar{b}$  remains as the leading discovery channel, due to three facts: (i) the branching ratio for  $\ell\nu bbbbjj$  final states slightly decreases with  $m_T$ ; (ii) for heavier T, the charged lepton from the semileptonic decay  $T\to W^+b\to \ell^+\nu b$  (or the charge conjugate) generically has a very large transverse momentum, what can be exploited to reduce backgrounds very efficiently [34]; (iii) larger T masses can only be explored at the high luminosity LHC run, where b tagging performance is degraded ans multi-jet backgrounds to the  $T\bar{t}H$  signal are larger. Preliminary studies have shown that for  $m_T=1$  TeV the significance achieved is  $S/\sqrt{B}\lesssim 3$  for 300 fb<sup>-1</sup>, and the  $\ell\nu bbbbjj$  channel cannot compete with the  $W^+bW^-\bar{b}$  mode, in which  $S/\sqrt{B}=9.1$ 

# Acknowledgements

I thank F. del Aguila and R. Pittau for useful discussions and for reading the manuscript. This work has been supported by FCT through grant SFRH/BPD/12603/2003 and by a MEC Ramon y Cajal contract.

## References

- [1] P. W. Higgs, Phys. Rev. Lett. 13 (1964) 508; Phys. Rev. 145 (1966) 1156.
- [2] R. Barate *et al.* [LEP Working Group for Higgs boson searches], Phys. Lett. B **565** (2003) 61
- [3] LEP Electroweak Working group hep-ex/0511027; see also http://lepewwg.web.cern.ch/LEPEWWG
- [4] N. Cabibbo, L. Maiani, G. Parisi and R. Petronzio, Nucl. Phys. B 158 (1979) 295
- [5] ATLAS detector and physics performance technical design report, CERN-LHCC-99-15
- [6] CMS technical proposal, CERN-LHCC-94-38
- [7] C. R. Chen, K. Tobe and C. P. Yuan, hep-ph/0602211

- [8] F. del Aguila, G. L. Kane and M. Quiros, Phys. Rev. Lett. 63 (1989) 942; F. del
   Aguila, L. Ametller, G. L. Kane and J. Vidal, Nucl. Phys. B 334 (1990) 1
- [9] N. Arkani-Hamed, A. G. Cohen and H. Georgi, Phys. Lett. B 513 (2001) 232; N. Arkani-Hamed, A. G. Cohen, E. Katz and A. E. Nelson, JHEP 0207 (2002) 034
- [10] E. A. Mirabelli and M. Schmaltz, Phys. Rev. D 61 (2000) 113011; S. Chang, J. Hisano, H. Nakano, N. Okada and M. Yamaguchi, Phys. Rev. D 62 (2000) 084025;
  F. del Aguila and J. Santiago, Phys. Lett. B 493 (2000) 175
- [11] P. H. Frampton, P. Q. Hung and M. Sher, Phys. Rept. 330 (2000) 263
- [12] J. A. Aguilar-Saavedra, Phys. Lett. B 625 (2005) 234 [Erratum-ibid. B 633 (2006) 792]
- [13] F. del Aguila and M. J. Bowick, Nucl. Phys. B 224 (1983) 107
- [14] P. Langacker and D. London, Phys. Rev. D 38 (1988) 886
- [15] V. D. Barger, M. S. Berger and R. J. N. Phillips, Phys. Rev. D 52 (1995) 1663
- [16] J. A. Aguilar-Saavedra, Phys. Rev. D 67 (2003) 035003 [Erratum-ibid. D 69 (2004) 099901]
- [17] LEP Electroweak Working Group, Results Summer 2004: M. Grünewald, http://lepewwg.web.cern.ch/LEPEWWG/stanmod/summer2004\_results
- [18] F. del Aguila and R. Pittau, Acta Phys. Polon. B **35** (2004) 2767
- [19] F. del Aguila, J. A. Aguilar-Saavedra and R. Miquel, Phys. Rev. Lett. 82 (1999) 1628
- [20] G. Azuelos et al., Eur. Phys. J. C **39S2** (2005) 13
- [21] T. Sjostrand, P. Eden, C. Friberg, L. Lonnblad, G. Miu, S. Mrenna and E. Norrbin, Comput. Phys. Commun. 135 (2001) 238
- [22] M. L. Mangano, M. Moretti, F. Piccinini, R. Pittau and A. D. Polosa, JHEP **0307** (2003) 001; See also http://mlm.home.cern.ch/m/mlm/www/alpgen/
- [23] S. Jadach, Z. Was, R. Decker and J. H. Kuhn, Comput. Phys. Commun. 76 (1993) 361
- [24] E. Barberio, B. van Eijk and Z. Was, Comput. Phys. Commun. 66 (1991) 115
- [25] E. Richter-Was, D. Froidevaux and L. Poggioli, ATL-PHYS-98-131

- [26] E. Murayama, I. Watanabe and K. Hagiwara, KEK report 91-11, January 1992
- [27] T. Stelzer and W. F. Long, Comput. Phys. Commun. 81 (1994) 357
- [28] B. P. Kersevan and E. Richter-Was, hep-ph/0405247
- [29] G. P. Lepage, CLNS-80/447
- [30] H. L. Lai et al. [CTEQ Collaboration], Eur. Phys. J. C 12 (2000) 375
- [31] R. Barate et al. [ALEPH Collaboration], Phys. Rept. 294 (1998) 1
- [32] B. P. Kersevan and E. Richter-Was, Eur. Phys. J. C 25 (2002) 379
- [33] A. D. Martin, R. G. Roberts, W. J. Stirling and R. S. Thorne, Phys. Lett. B 604 (2004) 61
- [34] J. A. Aguilar-Saavedra, hep-ph/0603199